Ionization Balance in Inertial Confinement Fusion Hohlraums

S. H. Glenzer, K. B. Fournier, B. G. Wilson, R. W. Lee, and L. J. Suter

L-447, Lawrence Livermore National Laboratory, University of California, P.O. Box 808, Livermore, California 94551

(Received 22 December 2000; published 5 July 2001)

We present the first x-ray spectroscopic measurements of the ionization balance in inertial confinement fusion hohlraums supported by 4ω Thomson scattering diagnostics. The experimental data show agreement with non-LTE radiation-hydrodynamic calculations of the averaged Au charge state and electron temperatures. These findings are consistent with the successful integrated modeling of the hohlraum radiation fields. Comparisons with detailed synthetic spectra calculations show that the experimental ionization distribution is slightly shifted indicating nonsteady state kinetics.

DOI: 10.1103/PhysRevLett.87.045002 PACS numbers: 52.57.–z, 52.25.Jm, 52.50.Jm, 52.70.La

Calculations of the ionization balance of highly ionized plasmas comprise an important research area for laboratory and astrophysical plasma studies. The x-ray emission spectra from these highly ionized atoms are used for the diagnostics of high temperature fusion plasmas, solar flares, and short-wavelength plasma light sources. In particular, in indirect drive inertial confinement fusion (ICF) research, the averaged ionization state $\bar{Z}$ is an important parameter because it determines basic physical quantities [1], i.e., acoustic velocities, electron densities, collision rates, and the thermal conductivity of the plasma, and is therefore closely linked to the understanding of the energetics of fusion plasmas.

In the indirect-drive approach to ICF [2], high-Z hohlraums are heated with intense laser or ion beams and used as radiation enclosures to drive the implosion of a fusion capsule with soft x rays. Calculating the total flux [3] and spectrum [4] of soft x rays is directly related to the ionization balance in the high-Z wall plasma [5]. Because of the vast number of atomic states that must be included into the calculation of the radiation equilibrium, accurate experiments are essential to guide the theoretical treatment of such high-Z plasmas. This applies particularly to gas-filled hohlraums, the present baseline design for indirect drive ICF experiments, where the radiation field and hot electrons must be included into the detailed spectra modeling. In addition, testing radiation-hydrodynamic modeling of the ionization balance is further motivated by the fact that laser scattering losses by stimulated Brillouin scattering and stimulated Raman scattering (SRS) [6] are known to be sensitive to the averaged charge state $\bar{Z}$ of the plasma [7]. The growth of these parametric instabilities depends on the damping of ion acoustic waves in the plasma which is determined by collisions and by the acoustic velocity and therefore related to the *local* value of $\bar{Z}$ in the plasma.

In this Letter, we present the first measurements of the ionization distribution in closed-geometry ICF hohlraums. The distribution is inferred from x-ray spectroscopic measurements (e.g., [8]) of the Au M-shell 5-3 transitions in the energy range of $3.3 < E < 3.6$ keV. The diagnostic value of these transitions had been first proposed when the lines were identified [9–11] and established when they had subsequently been analyzed with the unresolved transition array model [12–14]. Recently the nonlocal thermodynamic equilibrium (non-LTE) synthetic spectra modeling of these transitions was experimentally verified using open geometry disk plasmas [15]. In this study, the x-ray spectroscopic measurements were supported by ultraviolet Thomson scattering (TS) giving the electron temperature, T_e, of the plasma [16], as well as by diode measurements of the radiation field, $T_{\rm rad}$, and by bremsstrahlung measurements of the hot electron fraction, $f_{\rm hot}$, and energy, $E_{\rm hot}$. We find good agreement between the experimental data ($\bar{Z}$ and T_e) and non-LTE radiation-hydrodynamic modeling using the code LASNEX [3]. Consistent with the correct calculation of these microscopic parameters we find that the LASNEX simulations successfully model the overall radiation production of these hohlraums and show good agreement with the experimental radiation temperature measurements.

Moreover, our data set has further allowed us, for the first time, to test detailed synthetic spectra modeling for hohlraum plasma conditions. Using the independently measured hohlraum plasma parameters (T_e, $T_{\rm rad}$, $f_{\rm hot}$, $E_{\rm hot}$) as input into the synthetic spectra calculations results in an ionization distribution that is slightly narrower than inferred from the experimental x-ray spectra and with an averaged charge number 2% lower than the experiment. The inclusion of the hohlraum radiation field and of hot electron excitation only slightly increases the abundance of the more highly ionized atoms. Calculations indicate that non-steady-state kinetics is a possible explanation for the shortcomings of the present modeling.

We have used the Nova Laser Facility [17] to heat the hohlraums with ten 3ω (351 nm) laser beams with a total energy of 27 kJ. The hohlraums were 2750 μm long with a radius of 800 μm (scale-1) which is the standard size for capsule implosions [18] and present benchmarking experiments [19]. We have applied kinoform phase plates to smooth the laser beams and employed shaped laser pulses of 2.4 ns duration with a 7 TW foot reaching 17 TW peak power at 1.6 ns (pulse shape No. 22: PS22). The hohlraums were filled with 1 atm of propane (C_3H_8) to tamp the hohlraum wall plasma, and the diagnostic

and laser entrance holes (LEHs) have been covered with 0.35 μm thick polyimide. The radiation-hydrodynamic modeling shows that the C_3H_8 gas fill slows down the Au blowoff plasma resulting in a fairly homogeneous Au plasma close to the hohlraum walls.

A flat crystal x-ray spectrometer [20] has been employed to measure the Au M-shell 5-3 transitions through a 400 μm $\times$ 400 μm diagnostic hole cut in the side of the hohlraum (cf. Fig. 1). The spectrometer has been coupled to a gated microchannel plate detector [21] giving spectra with a temporal resolution of 150 ps and a wavelength resolution is $\lambda/\Delta\lambda \approx 600$.

Simultaneously we have measured the hohlraum electron temperatures in the gold and in the gas plasma with 4ω TS [22]. We have employed a 4ω probe laser with an energy of 50 J. The probe was focused to a cylindrical scattering volume with a diameter of $\sim$80 μm that is sufficiently small to probe the Au blowoff plasma. The scattering angle has been chosen to be 90° and the scattered TS light has been observed through the same diagnostic hole that has been used for the x-ray measurements. A 1-m spectrometer with an optical S-20 streak camera was used to detect the TS spectra with a temporal resolution of 100 ps and a wavelength resolution of 0.1 nm.

The hohlraum soft x-ray production was measured with a photoconductive detector (PCD) providing a radiation temperature measurement through the LEH (1200 μm diameter) at a polar angle of 25° [23]. In this study, we find peak values of $T_{\mathrm{rad}} = 190$ eV $\pm$ 20 eV. The hot electron fraction and energy has been inferred from bremsstrahlung and SRS measurements showing peak fractions of $f_{\mathrm{hot}} = 10\%$ with $E_{\mathrm{hot}} = 20$ keV.

Although it has been shown in the past that TS can, in principal, be employed for a *local* diagnostic of the averaged ionization state $\bar{Z}$ of a plasma [22], in this study, TS was applicable only for electron temperature diagnostics. Present probe laser technology limits TS measurements in gas-filled hohlraums to the observation of the ion feature which shows two ion acoustic wave resonances whose wavelength separation is determined by the ion acoustic wave dispersion relation. In the highly ionized Au plasma (with $T_i/T_e < 1$) the wavelength separation is proportional to $\sqrt{\bar{Z}T_e}$. The additional T_e measurement with the electron feature would be required to infer $\bar{Z}$ from TS alone [22]. For that reason, we use x-ray spectroscopy with the added advantage that it measures the distribution of charge states in the plasma.

Figure 2 shows spectroscopic measurements of the Au 5-3 transitions in the energy range $3.3 < E < 3.6$ keV (a) and a TS spectrum at 263 nm (b). Both measurements have been performed at the peak of the heater beam pulse ($t = 1.6$ ns). The x-ray data are composed of the $5f$-$3d$ transition arrays in Ge-like to Fe-like gold [15]. Using the HULLAC suite of codes [24] to fit the line emission from the various ionization states provides an estimate of their

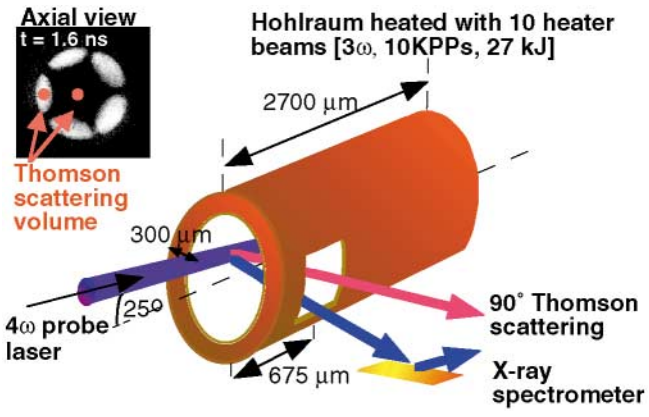

FIG. 1 (color). Schematic of the experiment. X-ray and 4ω TS spectra have been measured through a diagnostic hole in the side of the hohlraum. The locations of the TS volume are indicated on the gated 2D x-ray image that shows the emission of the Au blowoff plasma with $E > 2$ keV at 1.6 ns.

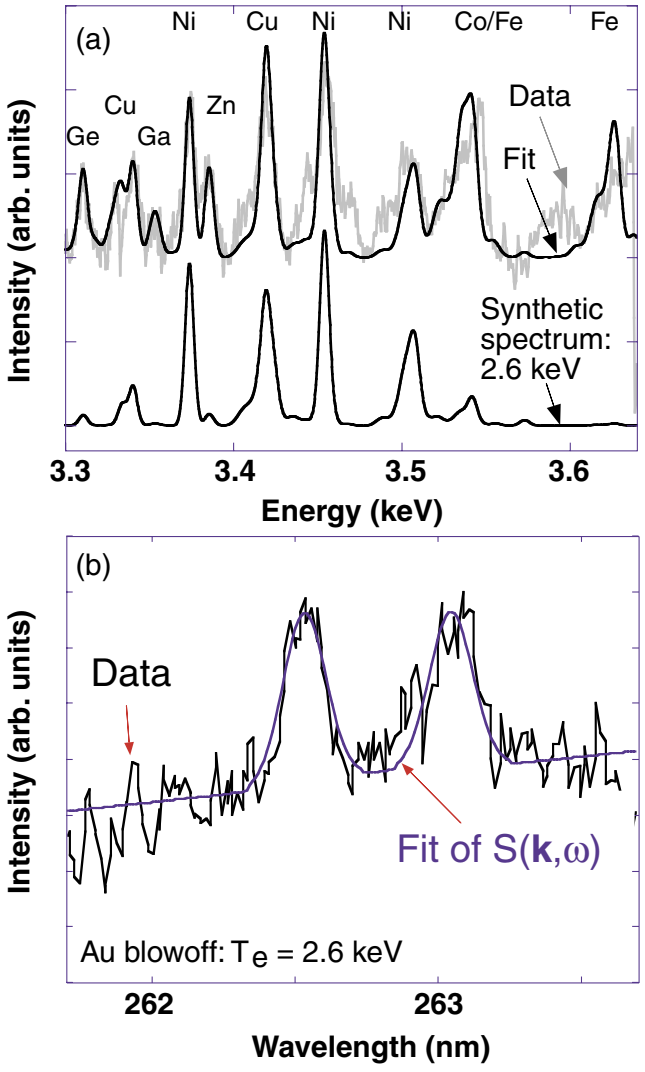

FIG. 2 (color). X-ray (a) and 4ω Thomson scattering data (b) along with theoretical spectra. In (a) the fit results into $\bar{Z} = 51$ and the synthetic spectra modeling for $T_e = 2.6$ keV gives $\bar{Z} = 50.5$. In (b) the frequency separation of the two ion acoustic peaks gives $T_e = 2.6$ keV.

abundance in the plasma giving $\bar{Z} = 51$, which was used to analyze the TS data. Figure 2 shows a least-squares fit to the TS spectrum by applying the theoretical form factor $S(\mathbf{k}, \omega)$ from Ref. [22]. As can be seen, the spectrum can be fit rather well by assuming scattering on a pure gold plasma where the width of the ion acoustic peaks is determined by the instrument function and modest velocity gradients in the Au plasma. When pointing the probe laser into the gas plasma, we observe broad heavily damped ion acoustic peaks (e.g., Ref. [22]) different from the spectrum shown in Fig. 2(b). For our conditions, the fit is not sensitive to the choice of the electron density and ion temperature and therefore we use parameters from the radiation-hydrodynamic modeling, $n_e = 1.4 \times 10^{21}$ cm^{-3} and $T_i = 0.8$ keV, respectively. We obtain $T_e = 2.6$ keV. By varying the fits within the noise of the data and by deconvolving spectral blends for Ge-, Ga-, and Co-like x-ray features have resulted into a 2% error bar for $\bar{Z}$ and a 10% error bar for T_e.

In Fig. 3 we compare the measured plasma parameters with non-LTE radiation-hydrodynamic LASNEX modeling. Two calculations have been performed. The first one uses a standard flux limited heat transfer model while the second

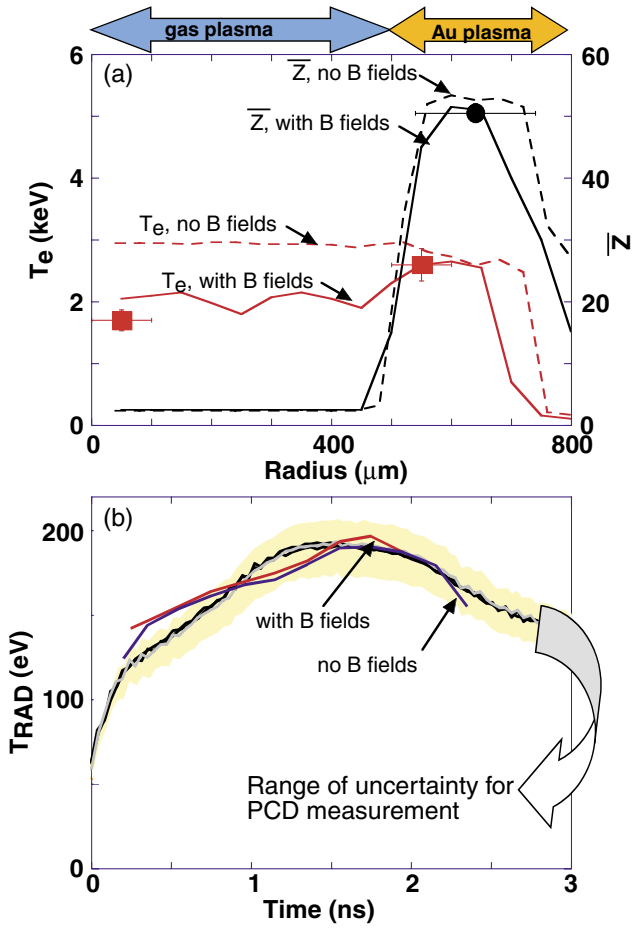

FIG. 3 (color). Comparison of the measured microscopic plasma parameters, T_e (squares) and $\bar{Z}$ (●) both measured at $t = 1.6$ ns (a), and of the soft x-ray production, $T_{\rm rad}$ (b), with non-LTE radiation-hydrodynamic LASNEX modeling.

calculation has used the model of Ref. [22] that includes a self-consistent calculation of magnetic fields and their effects on electron thermal transport. The latter also includes dielectronic recombination but similar to our earlier findings the effects on the calculated plasma conditions are small while the plasma is hot and heated by kilojoule laser beams. For both models, the comparison with the experimental plasma parameters $\bar{Z}$ and T_e shows good agreement in the Au plasma [Fig. 3(a)]. However, in the gas plasma TS shows that T_e decreases which is more consistent with the magnetic field modeling that calculates low temperatures in this region inside the hohlraum. In the gas plasma the flux limiter model predicts isotropic temperatures not in agreement with the TS measurements.

However, the soft x-ray radiation field in hohlraums is essentially determined by the conditions in the Au blowoff plasma. We find that both models calculate nearly the same radiation temperatures. Figure 3(b) shows a comparison between the non-LTE radiation-hydrodynamic modeling and PCD data from four identical experiments. The PCD measurements are very reproducible and nearly overlay with each other. The LASNEX results show agreement with the experiments and are well within the range of uncertainty of the measurement which is determined by the calibration error on the diode.

Although the averaged ionization state $\bar{Z}$ and consequently the hohlraum radiation field are well calculated by the LASNEX modeling, we find that the experimental ionization balance is not as well understood. This is indicated in Fig. 2(a) which compares the experimental spectrum with a fit using HULLAC and with a calculated synthetic spectrum for the temperature and density of the experiment. The latter spectrum has been obtained by first applying the code RIGEL to determine the steady-state gold ionization balance with a Monte Carlo method [25] and a screened hydrogenic atomic model. The ionization distribution obtained in this way has subsequently been post-processed with HULLAC calculating the individual spectral lines that belong to the various ionization stages. Dielectronic recombination and radiation transport have been included into the modeling but the latter has only a small effect on the simulated intensities of order 5% for our conditions. Although the Cu- and Ni-like spectral features are well reproduced, the abundances of the lower ionized atoms, i.e., Ge-like ($Z = 47$) and Ga-like ($Z = 48$) and of the higher ionized atoms, i.e., Co-like ($Z = 52$) and Fe-like ($Z = 53$) gold, are underestimated [cf. Fig. 2(a)].

Since emission spectroscopy provides spectra that are averaged along the line of sight we have examined the effect of modest plasma gradients on the spectrum. We find that the high intensity of the Ge-like and Ga-like features can be explained by small gradients in the gold blowoff such as those shown in Fig. 3(a) and by the fact that these features are rather weak and blended. On the other hand, the high abundance of Co- and Fe-like gold cannot be explained by gradients. Since Ni-like gold is a closed shell a significant increase in T_e to more than 3.5 keV is

required to produce these ions. This is not consistent with the simulations [Fig. 3(a)].

Figure 4 compares the experimental distribution of the Au charge states that is inferred from the fit of the spectrum [Fig. 2(a)] with the RIGEL calculations. Three calculations are shown: The first uses the electron temperature of 2.6 keV from TS and an electron density of $n_e = 1.4 \times 10^{21}$ cm^{-3} from LASNEX to calculate the ionization equilibrium. The second calculation includes excitation by hot electrons that are produced by SRS. The third calculation also includes excitation of atomic levels by the soft x-ray radiation field. We observe that including these effects shifts the distribution slightly to a higher averaged charge stage without affecting the width of the distribution. However, even the most sophisticated calculation with an upper limit for $T_{\rm rad}$ of 210 eV falls short in reproducing the experimental abundance of the more higher ionized atoms, i.e., Co-like ($Z = 52$) and Fe-like ($Z = 53$) gold. The calculated distribution is shifted by about one charge number to lower ionization stages.

Because we have ruled out high temperatures of order 3.5 keV in the Au blowoff plasma, we have used steady-state HULLAC simulations to estimate the effect of higher plasma densities on the spectrum. We find that an electron density of $n_e = 10^{22}$ cm^{-3} is required to reproduce the experimental abundance of Co- and Fe-like atoms. These high densities together with kilovolt temperatures in the gold plasma occur early ($t \approx 0.5$ ns) in the laser heating pulse. Later in the pulse at $t = 1.6$ ns, small plasma regions with such high densities occur at a lower temperature and ionization stage behind the large-scale gold plasma shelf of 150 μm length and $n_e = 1.4 \times 10^{21}$ cm^{-3} giving only a small contribution to the emission spectrum. These findings indicate that deviations from steady state might be required to explain the high Co- and Fe-like abundance at later times during the heating of the hohlraum.

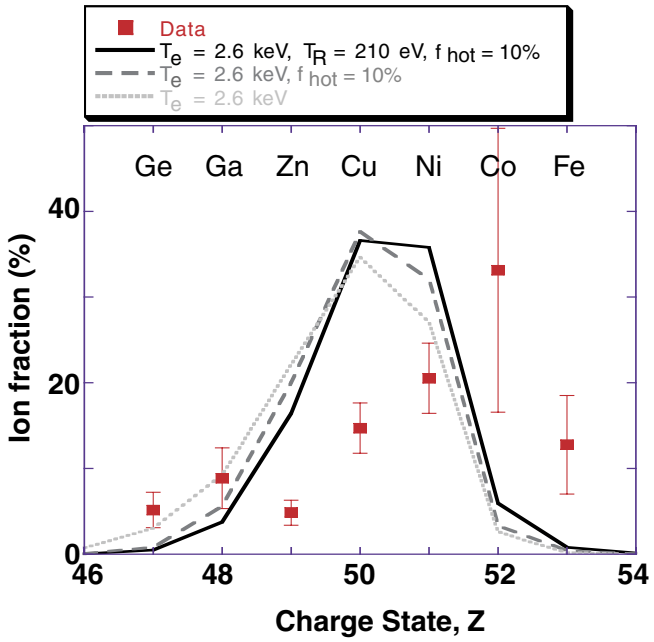

FIG. 4 (color). Comparison of the measured ionization distribution with detailed modeling using the code RIGEL.

In summary, we have presented a unique data set that has allowed us to test radiation-hydrodynamic modeling, as well as detailed calculations of atomic spectra for high-Z hohlraum plasmas. We find a consistent model for the formation of the Au wall plasma in hohlraums showing that the radiation temperature of 190 eV is consistent with an averaged ionization state of $\bar{Z} = 51$. However, using the electron temperature from TS, we find that the experimental ionization distribution is shifted to a higher charge state compared to the detailed atomic physics simulations. These results indicate the importance of developing non-steady-state kinetic codes for high-Z plasmas to better understand the x-ray production and radiative properties of hot dense matter such as encountered in ICF plasmas.

We thank B. A. Hammel, O. L. Landen, and B. J. MacGowan for discussions. This work was performed under the auspices of the U.S. Department of Energy by University of California Lawrence Livermore National Laboratory under Contract No. W-7405-ENG-48.

[1] M. Klapisch *et al.,* Phys. Plasmas **8**, 1817 (2001).
[2] J. D. Lindl, Phys. Plasmas **2**, 3933 (1995).
[3] L. J. Suter *et al.,* Phys. Rev. Lett. **73**, 2328 (1994); L. J. Suter *et al.,* Phys. Plasmas **3**, 2057 (1996).
[4] C. A. Back *et al.,* J. Quant. Spectrosc. Radiat. Transfer **51**, 19 (1994).
[5] J. R. Albritton and B. G. Wilson, Phys. Rev. Lett. **83**, 1594 (1999).
[6] W. L. Kruer, *The Physics of Laser Plasma Interactions* (Addison-Wesley, New York, 1988).
[7] R. K. Kirkwood *et al.,* Phys. Rev. Lett. **77**, 2706 (1996).
[8] A. A. Hauer, N. D. Delamater, and Z. M. Koenig, Laser Part. Beams **9**, 3 (1991).
[9] P. G. Burkhalter, C. M. Dozier, and D. J. Nagel, Phys. Rev. A **15**, 700 (1977).
[10] P. Audebert *et al.,* Phys. Rev. A **32**, 409 (1985).
[11] M. Busquet *et al.,* Phys. Scr. **31**, 137 (1985).
[12] C. Bauche-Arnoult *et al.,* Phys. Rev. A **33**, 791 (1986).
[13] J.-F. Wyart *et al.,* Phys. Rev. A **34**, 701 (1986).
[14] M. Busquet *et al.,* Phys. Rev. E **61**, 801 (2000).
[15] M. E. Foord *et al.,* Phys. Rev. Lett. **85**, 992 (2000).
[16] H.-J. Kunze, in *Plasma Diagnostics,* edited by W. Lochte-Holtgreven (North-Holland, Amsterdam, 1968), p. 550.
[17] E. M. Campbell *et al.,* Laser Part. Beams **9**, 209 (1991).
[18] B. A. Hammel *et al.,* Phys. Rev. Lett. **70**, 1263 (1993).
[19] R. E. Turner *et al.,* Phys. Plasmas **7**, 333 (2000).
[20] C. A. Back *et al.,* Rev. Sci. Instrum. **66**, 764 (1995).
[21] J. D. Kilkenny, Laser Part. Beams **9**, 49 (1991).
[22] S. H. Glenzer *et al.,* Phys. Plasmas **6**, 2117 (1999).
[23] C. Decker *et al.,* Phys. Rev. Lett. **79**, 1491 (1997).
[24] J. Oreg, W. H. Goldstein, M. Klapisch, and A. Bar-Shalom, Phys. Rev. A **44**, 1750 (1991).
[25] B. G. Wilson *et al.,* in *Radiative Properties of Hot Dense Matter,* edited by W. Goldstein, C. Hooper, J. Gauthier, J. Seely, and R. Lee (World Scientific, Singapore, 1991).